# Linear Dynamics and Control of a Kinematic Wobble–Yoke Stirling Engine

Alvarez–Aguirre, Alejandro; García–Canseco, Eloísa; Scherpen, Jacquelien M.A.

*Published in:*
49th IEEE Conference on Decision and Control



*Publication date:*
2010

49th IEEE Conference on Decision and Control
December 15-17, 2010
Hilton Atlanta Hotel, Atlanta, GA, USA

# Linear Dynamics and Control of a Kinematic Wobble–Yoke Stirling Engine

Alejandro Alvarez–Aguirre, Eloísa García–Canseco and Jacquelien M.A. Scherpen

*Abstract*— **This paper presents a control systems approach for the modeling and control of a kinematic wobble–yoke Stirling engine. The linear dynamics of the Stirling engine are analyzed based on the dynamical model of the system, developed by the authors in [1]. We show that the Stirling engine can be viewed as a closed–loop system, where the feedback control law is given by the pressure variations in the pistons. Since the closed–loop system exhibits unstable dynamics, we design a pre–compensator to stabilize the displacements of the engine's pistons, and an observer to estimate their piston velocities.**

## I. INTRODUCTION

Energy savings and concern for the environment and climate are major issues nowadays within our society. Due to this fact, in recent decades there has been an enormous interest in the application of heat engines for converting different types of heat source into electrical energy [2], [3].

One of the most promising applications is micro–combined heat and power (CHP) generation, or in other words, the simultaneous production of heat and power at a small–scale [4]. A micro–CHP consists of a gas engine which drives an electrical generator. The main purpose of a micro–CHP system is to replace the conventional boiler in a central heating system. Coal and natural gas power plants lose as waste heat two–thirds of the energy they produce [5]. With the use of micro–CHP units, this waste heat can be captured and used locally. The waste heat from the engine can be used in the heating system and the electricity generated can be either used in the house or exported to the grid in order to be consumed by the neighbors [4]. Supplying electricity back to the grid raises important economical and research/scientific challenges [3] which are not within the scope of this paper.

Micro–CHP systems can attain a similar conversion efficiency from gas to useful heat as a conventional boiler, typically around $80\%$. However, in addition, around $10-15\%$ can be converted to electricity. Among the technologies that have been proposed for micro–CHP applications we can mention fuel cells, internal combustion engines and Stirling engines [4], [6].

Theoretically, Stirling engines seem to be the most efficient device for converting heat into mechanical work, with high efficiencies, requiring high–temperatures [7]. Stirling engines are generally externally heated engines. Therefore, most sources of heat can be used to drive them. A curious paradox of Stirling engines is that they are at the same time well known and unknown [8]. They are well known because since their invention by Robert Stirling in 1816, they have been heavily studied, with an increasing interest during the last decades. There is no lack of literature references concerning the general and detailed aspects of Stirling technology, nevertheless, most of the studies rely on thermodynamics methods and intuitive design techniques. There exist, however, few literature on the application of dynamics and control methods to investigate their stability and dynamic properties, see for instance [9]–[13] and the recent work [14]. Moreover, most of the works analyze free–piston Stirling engines.

In this work, we focus on a Whispergen micro–CHP unit with Stirling engine technology, available at the Laboratory of Discrete Technology and Production Automation at the University of Groningen. This micro–CHP unit, developed by WhisperTech Limited [15], was originally designed as a battery charger for marine applications [16]. In contrast with most Stirling engines based on free–piston mechanisms, the Whispergen micro–CHP unit comprises a "wobble–yoke Stirling engine mechanism", that is, a four–cylinder double–acting Stirling engine configuration whose design is based on the classical spherical four–bar linkage [17].

Based on the nonlinear dynamical model of the wobble–yoke Stirling engine, developed by the authors in [1], we analyze the linear dynamics of the engine. Our contributions are twofold. First, we show that the Stirling engine is an unstable closed–loop system where the state feedback is given by the pressure variations in the pistons. Although a similar approach has been followed by [14], [18] for the study of free–piston Stirling engines, to the best of the authors knowledge, none of the previous works concerns the kinematic wobble–yoke Stirling engine. Second, using the fact that working gases in piston engines, behave as linear mass–spring systems, we use linear control tools to design a pre–compensator that ensures stability of the pistons' displacements and an observer to estimate the piston velocities.

## II. DESCRIPTION OF THE SYSTEM

Figure 1 shows the schematic representation of the four–cylinder double–acting Stirling engine. The four cylinders are phased at $90^o$ from each other with respect to $\phi$. The links connecting the cylinders form the wobble–yoke mechanism whose function is to translate the vertical motion of the cylinders into the rotational motion through the shaft angle $\phi$. The design of the wobble yoke mechanism is based on the classical spherical four–bar linkage [17]. These kind

This work was partially supported by the Mexican Council for Science and Technology (CONACyT) and by the Mexican Ministry of Education (SEP).

Alejandro Alvarez–Aguirre is with the Dynamics and Control Group, Faculty of Mechanical Engineering, Eindhoven University of Technology, PO Box 513, 5600 MB Eindhoven, The Netherlands. a.a.alvarez@tue.nl

Eloísa García–Canseco is with the Control Systems Technology Group, Faculty of Mechanical Engineering, Eindhoven University of Technology, PO Box 513, 5600 MB Eindhoven, The Netherlands. e.garcia.canseco@tue.nl

Jacquelien M.A. Scherpen is with the Faculty of Mathematics and Natural Sciences, ITM, University of Groningen, Nijenborgh 4, 9747 AG, Groningen, The Netherlands, j.m.a.scherpen@rug.nl

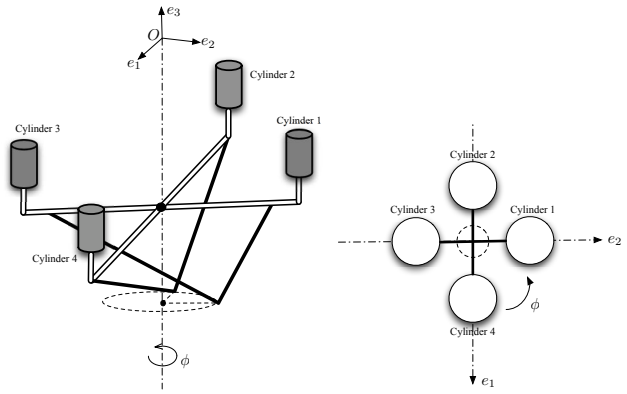


Fig. 1. Schematic representation and cylinders configuration of the wobble yoke Stirling engine.

of linkages, which are well known in robotics, have the property that every link in the system rotates about the same fixed point [19], [20]. Hence, as indicated by its name, the trajectories of the points at the end of each link lie on concentric spheres. In robotics, only the revolute joint is compatible with this rotational movement and its axis must pass through the fixed point. The wobble yoke is indeed a particular class of the spherical linkage known as *spherical crank rocker* [17]. In this case, the revolute joints are replaced by the spherical bearings located at points $b_1$, $b_3$, $c_1$ and $d$ (cf. Figure 2). The axis of the aforementioned bearings must intersect the sphere center $O$.

The working principle of this mechanism can be explained by referring to Figure 2. The mechanism is based on a beam which pivots about its center $O$ in one plane ($e_2e_3$ for beam 1, and $e_1e_3$ for beam 2). Each beam is attached to the cylinders with connecting rods at each end via bearings $a_1$ and $a_3$. An eccentric bearing $c_1$ is attached to the drive shaft and it is connected to the beam via two bearings $b_1$ and $b_3$. The eccentric bearing $c_1$ is the rotating part of the mechanism. When the engine is working, the vertical motion of the pistons inside the cylinders (not shown in Figure 2), induces a rotational movement on bearing $c_1$. Due to the geometrical and physical configuration of the mechanism, bearing $c_1$ describes a circle of radius $l_{c_1d}$. The axis of bearings $b_1$, $b_3$, $c_1$ and $d$ must intersect the center $O$, so that the kinematic constraints of the spherical crank rocker [19], [20] are satisfied. We also notice that the axis $l_{Oc_1}$ of bearing $c_1$ is perpendicular to the beam, i.e., $l_{Oc_1} \perp l_{b_1b_3}$. An analogous discussion applies to the second beam. We refer the reader to [16], [17] for more details about the wobble–yoke Stirling engine.

## III. DYNAMICAL MODEL

In this section we present a summary of the equations that characterize the dynamic behavior of the wobble–yoke Stirling engine, as developed by [1]. The definition of the parameters as well as their nominal values are summarized in Table I.

### A. Kinematics

It can be shown that the kinematic equation relating the beam angular displacement $\theta_j$, in terms of the crank angle $\phi$ are respectively given by [1], [17]

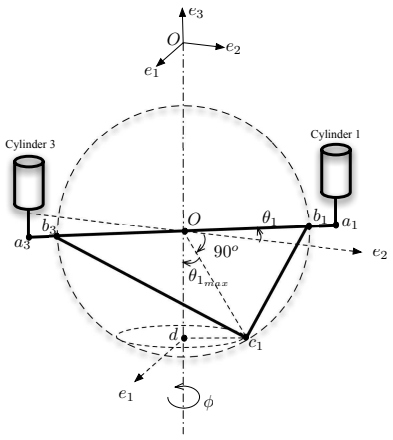


Fig. 2. Schematic picture of beam 1. $\theta_1$ is the angle between the beam and the axis $e_2$. The crank angle $\phi$ is measured in the counterclockwise direction from the positive axis $e_1$.

$$\boldsymbol{\theta} = \begin{bmatrix}\theta_1 \\ \theta_2\end{bmatrix} = \begin{bmatrix}\tan^{-1}(\kappa \sin\phi) \\ \tan^{-1}(\kappa \cos\phi)\end{bmatrix} \tag{1}$$

where $\kappa = \tan\theta_{1_{max}}$. Eq. (1) describes the working principle of the wobble–yoke mechanism as explained in Section II. For the vertical displacements $z_i$, we only have two independent equations, namely, $z_1$ and $z_2$ ($z_3 = -z_1$ and $z_4 = -z_2$). Therefore, we define the vector $\boldsymbol{z} = [z_1, z_2]^\top$, with $\boldsymbol{z} = l_{Oa_1}\boldsymbol{\theta}$.

### B. Dynamics of the pistons' motion

Consider the free–body diagram shown in Fig. 3. The dynamic equation for the vertical motion of the $i$–th piston is given by [1]

$$m\ddot{z}_i = (A_p - A_r)(p_{c_i} - p_{c_{i0}}) - A_p(p_{e_i} - p_{e_{i0}}) - k_{p_i}(z_i - z_{i0}) - b_{p_i}\dot{z}_i, \tag{2}$$

where $p_{c_{i0}}$ and $p_{e_{i0}}$ are the initial pressures in the compression and expansion spaces, respectively. The initial piston positions $z_{i0}$ correspond to the point of vertical static equilibrium, i.e., when the engine is not yet running.

According to the Schmidt analysis [21], the Stirling engine consist of five serially–connected components, namely, a compression space, cooler, regenerator, heater and expansion space. These five components constitute a thermodynamic cycle. In the case of the wobble–yoke Stirling engine, the engine is composed of four cycles [16], [17]. Each cycle consist of the compression space of cylinder $i$, the expansion space of cylinder $(i+1)$ and the connecting cooler, regenerator and heater between cylinders $i$ and $(i+1)$. Since the isothermal analysis does not account for pressure gradients, we assume no pressure drop across the cooler, regenerator and heater, and thus, the pressure in the compression space of the $i$ cylinder equals the pressure in the expansion space of the adjacent cylinder $(i+1)$ [16], [17] i.e.,

$$p_{e_1} = p_{c_4}, \quad p_{e_2} = p_{c_1}, \quad p_{e_3} = p_{c_2}, \quad p_{e_4} = p_{c_3}. \tag{3}$$

Recalling from Subsection III-A that $z_3 = -z_1$ and $z_4 = -z_2$, the dynamic equations of the piston motion (2), after substituting (3) become

$$m\ddot{z}_1 = (A_p - A_r)(p_{c_1} - p_{c_{10}}) - A_p(p_{c_4} - p_{c_{40}}) - k_{p_1}(z_1 - z_{10}) - b_{p_1}\dot{z}_1, \tag{4}$$

$$m\ddot{z}_2 = (A_p - A_r)(p_{c_2} - p_{c_{20}}) - A_p(p_{c_1} - p_{c_{10}}) - k_{p_2}(z_2 - z_{20}) - b_{p_2}\dot{z}_2, \tag{5}$$

TABLE I

SYSTEM PARAMETERS (NOMINAL VALUES SHOWN)

| *Symb.* | *Value* | *Description* |
|---|---|---|
| $a_i$ | | connecting rod bearing center, |
| $A_p$ | 0.0014 | piston area [$\mathrm{m}^2$] |
| $A_r$ | $2.4053 \times 10^{-4}$ | piston rod area [$\mathrm{m}^2$] |
| $b_i$ | | wobble yoke–beam bearing center, |
| $b_{p_i}$ | 10 | damping coefficient, |
| $c_j$ | | nutating bearing center, |
| $d$ | | crankshaft bearing center, |
| $e_n$ | | axes of the fixed reference frame, |
| $F_{(\cdot)}$ | | force [N], |
| $g$ | 9.81 | acceleration due to gravity [$\mathrm{m/s}^2$], |
| $h_s$ | 0.025 | stroke of the piston [m] |
| $I$ | 0.0135 | mass moment of inertia about the pivot $O$ [$\mathrm{kgm}^2$], |
| $k_{p_i}$ | 450 | piston spring constant [N/m], |
| $l_{Oa_1}$ | 0.0705 | distance [m], |
| $m$ | 0.4384 | piston assembly mass incl. the connecting rod [kg], |
| $m_T$ | 0.0015 | total mass of the working gas [kg], |
| $M_i$ | | angular momentum with respect to the axis $e_i$ [Nm], |
| $O$ | | center of the fixed reference frame, main pivot center, |
| $p_{c_i}$ | | pressure in compression space [$\mathrm{N/m}^2$], |
| $p_{cc}$ | | crankcase pressure [$\mathrm{N/m}^2$], |
| $p_{e_i}$ | | pressure in expansion space [$\mathrm{N/m}^2$], |
| $p_m$ | | mean pressure in the working space [$\mathrm{N/m}^2$], |
| $R$ | 8.3144 | gas constant [$\mathrm{J/(K \cdot mol)}$], |
| $T_h$ | 975 | hot end temperature [K], |
| $T_k$ | 360 | cold end temperature [K], |
| $T_r$ | 617.2632 | regenerator effective temperature [K], |
| $V_{dc}$ | $6.7512 \times 10^{-7}$ | dead volume in compression space [$\mathrm{m}^3$], |
| $V_{de}$ | $3.5918 \times 10^{-6}$ | dead volume in expansion space [$\mathrm{m}^3$], |
| $V_h$ | $9.1800 \times 10^{-6}$ | heater volume [$\mathrm{m}^3$], |
| $V_k$ | $8.2687 \times 10^{-6}$ | cooler volume [$\mathrm{m}^3$], |
| $V_{swc}$ | $2.8130 \times 10^{-5}$ | swept volume in compression space [$\mathrm{m}^3$], |
| $V_{swe}$ | $3.4143 \times 10^{-5}$ | swept volume in expansion space [$\mathrm{m}^3$], |
| $z_i$ | | vertical displacement [m], |
| $z_{i_{eq}}$ | | equilibrium length of the $i$–th piston spring [m], |
| $z_{max}$ | 0.0125 | maximum piston displacement=$h_s/2$ [m], |
| $\dot{z}_i$ | | velocity [m/s], |
| $\ddot{z}_i$ | | acceleration [$\mathrm{m/s}^2$], |
| $\theta_j$ | | beam angle [rad], |
| $\dot{\theta}_j$ | | beam angular velocity [rad/s], |
| $\ddot{\theta}_j$ | | beam angular acceleration [$\mathrm{rad/s}^2$], |
| $\theta_{j_{max}}$ | 0.1782 | maximum beam angle [rad], |
| $\phi$ | | crankshaft angle [rad], |
| $\tau$ | | shaft torque [Nm]. |

where the instantaneous pressure $p_{c_i}$ in the compression spaces in terms of the piston displacements $z_i$ is given by

$$p_{c_i} = p_m \left(1 + \frac{A_p - A_r}{2\beta_1 T_k} z_i - \frac{A_p}{2\beta_1 T_h} z_{i+1}\right)^{-1} \tag{6}$$

where $p_m = m_T R/\beta_1$ is the mean pressure in the working space and $\beta_1$ is a constant defined in Appendix (eq. (A.1)).

### C. Shaft torque

As mentioned in Section II, the wobble–yoke mechanism translates the vertical motion of the piston into rotational motion through the shaft angle $\phi$. The shaft torque equation is given by [1]

$$\tau = \frac{M_1 + M_2}{l_{Oa_1}} z_2, \tag{7}$$

where $M_1 = l_{Oa_1}(F_1 - F_3) - \frac{I}{l_{Oa_1}^2}\ddot{z}_1$ and $M_2 = l_{Oa_1}(F_2 - F_4) - \frac{I}{l_{Oa_1}^2}\ddot{z}_2$ are the angular momenta with respect to the pivot center $O$. The net forces $F_i$, acting at the connecting rod bearings $a_i$, $i = 1, \ldots, 4$ are defined as $F_i = m\ddot{z}_i$.

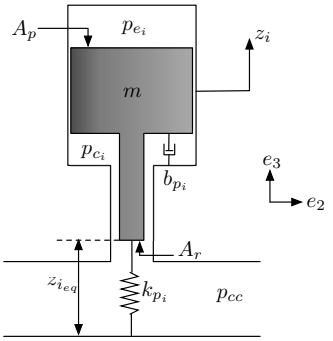


Fig. 3. Free–body diagram for the pistons of the Wobble Yoke Stirling engine.

## IV. LINEAR DYNAMICS

Because of the pressure dynamics (6), the piston motion equations (4) and (5) are nonlinear. However, since the working gas behaves like a linear spring [22], the system can be studied via linear analysis methods. For convenience, we linearize equation (6) around the initial piston positions $z_i = z_{i_0}$ and $z_{i+1} = z_{(i+1)_0}$ as follows[1]

$$p_{c_i} = p_{c_{i0}} + \left.\frac{\partial p_{c_i}}{\partial z_i}\right|_{\substack{z_i = z_{i0} \\ z_{i+1} = z_{(i+1)0}}} (z_i - z_{i0}) + \left.\frac{\partial p_{c_i}}{\partial z_{i+1}}\right|_{\substack{z_i = z_{i0} \\ z_{i+1} = z_{(i+1)0}}} (z_{i+1} - z_{(i+1)0}). \tag{8}$$

After some simplifications, equation (8) becomes

$$p_{c_i} = \frac{p_m}{\gamma_i}\left(1 - \frac{A_p - A_r}{2\beta_1\gamma_i T_k}(z_i - z_{i0}) + \frac{A_p}{2\beta_1\gamma_i T_h}(z_{i+1} - z_{(i+1)0})\right) \tag{9}$$

with the constant term $\gamma_i$ given by

$$\gamma_i = 1 + \frac{A_p - A_r}{2\beta_1 T_k} z_{i0} - \frac{A_p}{2\beta_1 T_h} z_{(i+1)0}.$$

Define $\tilde{z}_i = z_i - z_{i0}$ and $\tilde{p}_{c_i} = p_{c_i} - p_{c_{i0}}$. Then equations (4), (5) and (9) can be represented in state–space as:

$$\dot{\boldsymbol{x}} = \mathbf{A}\boldsymbol{x} + \mathbf{B}\boldsymbol{u}, \tag{10}$$

$$\boldsymbol{y} = \mathbf{C}\boldsymbol{x}, \tag{11}$$

where $\boldsymbol{x} = [\tilde{z}_1, \tilde{z}_2, \dot{\tilde{z}}_1, \dot{\tilde{z}}_2]^T \in \mathbb{R}^4$ is the state–space vector. The output vector $\boldsymbol{y} \in \mathbb{R}^p$ contains the variable we are interested in controlling, which are determined from the structure of the output matrix $\mathbf{C} \in \mathbb{R}^{p\times 4}$. The state matrix $\mathbf{A} \in \mathbb{R}^{4\times 4}$ and the input matrix $\mathbf{B} \in \mathbb{R}^{4\times 3}$ are respectively given by

$$\mathbf{A} = \begin{bmatrix} 0 & 0 & 1 & 0 \\ 0 & 0 & 0 & 1 \\ -\frac{k_{p_1}}{m} & 0 & -\frac{b_{p_1}}{m} & 0 \\ 0 & -\frac{k_{p_2}}{m} & 0 & -\frac{b_{p_2}}{m} \end{bmatrix},$$

[1]Although the binomial expansion, or equivalently, the linearization around zero initial piston positions, has been widely used in free–piston Stirling engines to linearize the pressure equation (6), in the kinematic wobble–yoke Stirling engine, the choice $z_i = z_{i+1} = 0$ is not possible due to the physical constraints of the engine.

$$\mathbf{B} = \begin{bmatrix} 0 & 0 & 0 \\ 0 & 0 & 0 \\ \frac{(A_p - A_r)}{m} & 0 & -\frac{A_p}{m} \\ -\frac{A_p}{m} & \frac{(A_p - A_r)}{m} & 0 \end{bmatrix}.$$

Using the linearized pressure equation (9), the input term $\boldsymbol{u} = \tilde{\boldsymbol{p}} = [\tilde{p}_{c_1}, \tilde{p}_{c_2}, \tilde{p}_{c_4}]^T \in \mathbb{R}^3$ can be written as the state feedback equation

$$\boldsymbol{u} = -\mathbf{K}\boldsymbol{x}, \tag{12}$$

with constant gain matrix $\mathbf{K} \in \mathbb{R}^{3\times 4}$

$$\mathbf{K} = \begin{bmatrix} \beta_2 & \beta_3 & 0 & 0 \\ \beta_4 & \beta_5 & 0 & 0 \\ \beta_8 & \beta_9 & 0 & 0 \end{bmatrix},$$

and constant terms $\beta_i$, $i = 2, \ldots 9$ defined in equations (A.2)–(A.7).

*Remark 1:* Figure 4 depicts the block diagram of the linearized system (10)–(12). It is worth noticing that the system (10) is self–excited via the input term $\boldsymbol{u}$ (12), which depends on the initial pressure and temperature conditions, so as to induce the engine operation. Therefore, as already pointed out by [14], [18], the Stirling engine can be viewed as a dynamical system subject to a state–feedback law (the pressure), which can be altered by manipulating the parameters of the system or by designing a suitable pre–compensator, as we will show in the next Section.

*Remark 2:* Figure 5 shows the root locus of the closed–loop system (10)–(12) as the viscous friction parameter $b_{p_i}$ varies. At the nominal value $b_{p_i} = 10$ Ns/m, the closed–loop poles are located at $12.3 \pm 87.11j$ and $-35.11 \pm 87.11j$. Due to the positive real part of two poles, the system is unstable and the piston displacement $z_i$ will oscillate with increasing amplitude.

*Remark 3:* Theoretically, the Stirling engine works in a stable cyclic steady–state, when the characteristic polynomial has two imaginary roots and two roots with a negative real part [23]. However, as depicted in Fig. 5, at the nominal values of the parameters, the root locus of the wobble–yoke Stirling engine, do not cross the imaginary axis.

## V. PRE–COMPENSATOR AND OBSERVER DESIGN

### A. Pre–compensator

From Figure 4 we observe that adding a pre–compensator $\boldsymbol{v}(\boldsymbol{x})$ modifies the system's input $\boldsymbol{u}$ so that besides the auto–excitation term, additional pressure is injected to the engine. Assuming that all components of the state vector $\boldsymbol{x}$ are measured, our control objective is to design a state feedback $\boldsymbol{v}(\boldsymbol{x})$ so that the new input

$$\boldsymbol{u}(\boldsymbol{x}) = -\mathbf{K}\boldsymbol{x} + \boldsymbol{v}(\boldsymbol{x}) \tag{13}$$

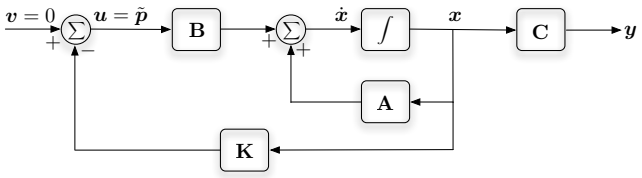


Fig. 4. Block diagram of the closed–loop system.

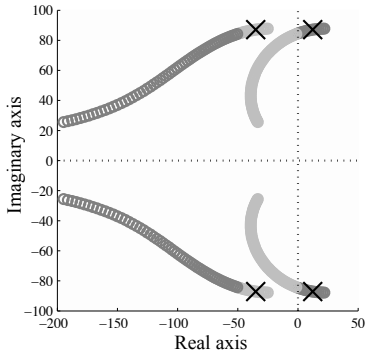


Fig. 5. Root–locus trajectories for varying values of $b_{p_i}$. The closed–loop poles for the nominal value $b_{p_i} = 10$ N·s/m are located at $12.3 \pm 87.11j$ and $-35.11 \pm 87.11j$.

ensures a stable piston oscillation at 30 Hz with a maximal amplitude of $z_{max} = h_s/2$. To this end, we set the control input as

$$\boldsymbol{u} = \boldsymbol{u}_r - \bar{\mathbf{K}}(\boldsymbol{x} - \boldsymbol{x}_r), \tag{14}$$

where $\boldsymbol{x}_r$ is the desired trajectory, $\boldsymbol{u}_r$ is a feedforward control input, and $\bar{\mathbf{K}}$ is an appropriate gain matrix, which can be chosen by pole placement. Solving (13) and (14) for $\boldsymbol{v}$ yields

$$\boldsymbol{v} = \boldsymbol{u}_r - \bar{\mathbf{K}}(\boldsymbol{x} - \boldsymbol{x}_r) + \mathbf{K}\boldsymbol{x}. \tag{15}$$

The new closed–loop system, after substituting (15) and (13) into (10) results in

$$\dot{\boldsymbol{x}} = (\mathbf{A} - \mathbf{B}\bar{\mathbf{K}})\boldsymbol{x} + \mathbf{B}\bar{\mathbf{K}}\boldsymbol{x}_r + \mathbf{B}\boldsymbol{u}_r. \tag{16}$$

Define the tracking error $\tilde{\boldsymbol{x}} = \boldsymbol{x} - \boldsymbol{x}_r$, then the error dynamics are obtained as

$$\dot{\tilde{\boldsymbol{x}}} = (\mathbf{A} - \mathbf{B}\bar{\mathbf{K}})\tilde{\boldsymbol{x}}, \tag{17}$$

where we have used

$$\dot{\boldsymbol{x}}_r = \mathbf{A}\boldsymbol{x}_r + \mathbf{B}\boldsymbol{u}_r \tag{18}$$

for the dynamics of the reference trajectory and feedforward generator. Equation (17) clearly shows that the tracking error will converge to zero provided a proper choice of the gain matrix $\bar{\mathbf{K}}$, done by pole placement. The block diagram representation in Figure 6 depicts the pre–compensator system as proposed so far.

*Remark 4:* To address the modeling and control of the engine from a control perspective, the pressure differences in the pistons' chambers have been chosen as the system's control inputs. Nevertheless, it is worth noting that the temperature variations along the rods connecting the pistons produce such pressure differences.

### B. Trajectory and feedforward generator

Since the pressure variation $\tilde{p}_{c_3}$ does not appear explicitly in the system equation (10), the feedforward term $\boldsymbol{u}_r$ cannot be directly computed from (18) by using the pseudo–inverse of $\mathbf{B}$. To take into account the effect of $\tilde{p}_{c_3}$, equation (2) is evaluated for the four pistons at the reference trajectories $\boldsymbol{x}_r$, resulting in

$$\boldsymbol{\Delta}_{u_{r_f}} \boldsymbol{u}_{r_f} = \boldsymbol{\Delta}_{\dot{x}_r} \dot{\boldsymbol{x}}_r + \boldsymbol{\Delta}_{x_r} \boldsymbol{x}_r, \tag{19}$$

where $\boldsymbol{u}_{r_f} = [\tilde{p}_{c_{1_r}}, \tilde{p}_{c_{2_r}}, \tilde{p}_{c_{3_r}}, \tilde{p}_{c_{4_r}}]^T$, and

$$\boldsymbol{\Delta}_{u_{r_f}} = \begin{bmatrix} A_p - A_r & 0 & 0 & -A_p \\ -A_p & A_p - A_r & 0 & 0 \\ 0 & -A_p & A_p - A_r & 0 \\ 0 & 0 & -A_p & A_p - A_r \end{bmatrix},$$

$$\boldsymbol{\Delta}_{\dot{x}_r} = \begin{bmatrix} b_{p_1} & 0 & m & 0 \\ 0 & b_{p_2} & 0 & m \\ -b_{p_1} & 0 & -m & 0 \\ 0 & -b_{p_2} & 0 & -m \end{bmatrix},$$

$$\boldsymbol{\Delta}_{x_r} = \begin{bmatrix} k_{p_1} & 0 & 0 & 0 \\ 0 & k_{p_2} & 0 & 0 \\ -k_{p_1} & 0 & 0 & 0 \\ 0 & -k_{p_2} & 0 & 0 \end{bmatrix}.$$

Solving (19) for $\boldsymbol{u}_{r_f}$ yields $\boldsymbol{u}_{r_f} = \boldsymbol{\Delta}_{u_{r_f}}^{-1}(\boldsymbol{\Delta}_{\dot{x}_r}\dot{\boldsymbol{x}}_r + \boldsymbol{\Delta}_{x_r}\boldsymbol{x}_r)$, from which the feedforward term $\boldsymbol{u}_r = [\tilde{p}_{c_{1_r}}, \tilde{p}_{c_{2_r}}, \tilde{p}_{c_{4_r}}]^T$ can be obtained.

### C. Observer design

The synthesis of the state–feedback pre–compensator presented in Subsection V-A considered that the state $\boldsymbol{x}$ was fully measured. However, from a practical viewpoint, the piston velocities cannot be directly measured, and thus, a reduced–order estimator is required.

Assume the state can be partitioned as $\boldsymbol{x} = [\boldsymbol{x}_a, \boldsymbol{x}_b]^T$, where $\boldsymbol{x}_a = [z_1, z_2]^T$ can be directly measured and $\boldsymbol{x}_b = [\dot{z}_1, \dot{z}_2]^T$ has to be estimated. According to this partition, equations (10)–(11) can be written as

$$\begin{bmatrix} \dot{\boldsymbol{x}}_a \\ \dot{\boldsymbol{x}}_b \end{bmatrix} = \begin{bmatrix} \mathbf{A}_{aa} & \mathbf{A}_{ab} \\ \mathbf{A}_{ba} & \mathbf{A}_{bb} \end{bmatrix} \begin{bmatrix} \boldsymbol{x}_a \\ \boldsymbol{x}_b \end{bmatrix} + \begin{bmatrix} \mathbf{B}_a \\ \mathbf{B}_b \end{bmatrix} \boldsymbol{u}, \tag{20}$$

$$\boldsymbol{y} = \boldsymbol{x}_a, \tag{21}$$

where $\mathbf{A}_{aa} = \mathbf{0}_{2\times 2}$, $\mathbf{A}_{ab} = \mathbf{I}_{2\times 2}$, $\mathbf{B}_a = \mathbf{0}_{2\times 3}$ and

$$\mathbf{A}_{ba} = \begin{bmatrix} \frac{\beta_8 A_p - \beta_2(A_p - A_r) - k_{p1}}{m} & \frac{\beta_9 A_p - \beta_3(A_p - A_r)}{m} \\ \frac{\beta_2 A_p - \beta_4(A_p - A_r)}{m} & \frac{\beta_3 A_p - \beta_5(A_p - A_r) - k_{p2}}{m} \end{bmatrix},$$

$$\mathbf{A}_{bb} = \begin{bmatrix} -\frac{b_{p_1}}{m} & 0 \\ 0 & -\frac{b_{p_2}}{m} \end{bmatrix}, \mathbf{B}_b = \begin{bmatrix} \frac{A_p - A_r}{m} & 0 & -\frac{A_p}{m} \\ -\frac{A_p}{m} & \frac{A_p - A_r}{m} & 0 \end{bmatrix}.$$

Consider the following estimator [24]

$$\dot{\hat{\boldsymbol{x}}}_b = (\mathbf{A}_{bb} - \mathbf{L}\mathbf{A}_{ab})\hat{\boldsymbol{x}}_b + \mathbf{A}_{ba}\boldsymbol{x}_a + \mathbf{B}_b\boldsymbol{u} + \mathbf{L}\dot{\boldsymbol{y}}, \tag{22}$$

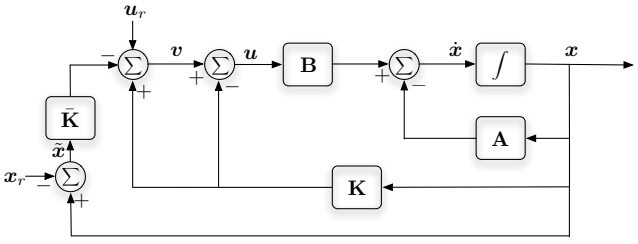


Fig. 6. Pre–compensator block diagram representation for the wobble–yoke Stirling engine.

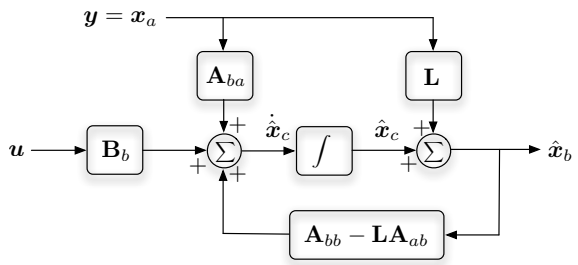


Fig. 7. Pre–compensator–estimator block diagram representation for the wobble–yoke Stirling engine.

where $\mathbf{L} \in \mathbb{R}^{2\times 2}$ is the estimator gain matrix. Define the new estimator state $\hat{\boldsymbol{x}}_c = \hat{\boldsymbol{x}}_b - \mathbf{L}\boldsymbol{y}$. Then, the dynamics of the reduced–order estimator (22) can be written as

$$\dot{\hat{\boldsymbol{x}}}_c = (\mathbf{A}_{bb} - \mathbf{L}\mathbf{A}_{ab})\hat{\boldsymbol{x}}_b + \mathbf{A}_{ba}\boldsymbol{x}_a + \mathbf{B}_b\boldsymbol{u}.$$

By defining the estimator error $\tilde{\boldsymbol{x}}_b = \boldsymbol{x}_b - \hat{\boldsymbol{x}}_b$, it can be shown that $\dot{\tilde{\boldsymbol{x}}}_b = (\mathbf{A}_{bb} - \mathbf{L}\mathbf{A}_{ab})\tilde{\boldsymbol{x}}_b$. Therefore, given an adequate choice of the gains in matrix $\mathbf{L}$, done by pole placement, the estimator error will converge to zero. A block–diagram representation of the reduced–order estimator is shown in Figure 7.

## VI. SIMULATION RESULTS

In order to illustrate the pre-compensator and observer designed for the Stirling engine, numerical simulations have been carried out by using the linear controller/observer in the original nonlinear model. The desired pistons displacements are sinusoids with phase difference of $\pi/2$, frequency of 30Hz and amplitude of $hs/2 = 0.0125$. The initial crankshaft angle is $\phi(0) = \pi/3$, resulting in the initial piston positions and velocities $\boldsymbol{x}(0) = [0.0109,\ 0.0063,\ 0,\ 0]^T$. On the other hand, the observer is initialized at $\hat{\boldsymbol{x}}_b = [0,\ 0]^T$. The desired closed-loop poles for the controller are located at $[-300, -300, -200, -200]$, whereas those of the estimator are located at $[-600, -400]$. The controller and observer gain matrices were chosen considering the following two requirements. First, a fast response without overshoot from the controller, in order to constrain the piston motion to their encasement while converging to their reference trajectories. Second, an even faster response from the observer so that the estimated estates emulate the system states in a very short period.

The plots in Figure 8 show the desired and real piston displacements (black and dashed gray, respectively) during time $t \in [4, 4.1]$s. while the resulting shaft torque is shown in Figure 9 for the same period.

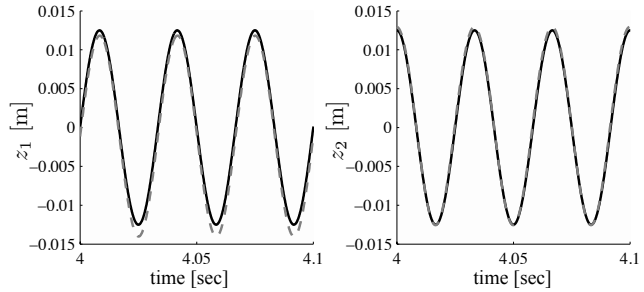


Fig. 8. Piston displacements

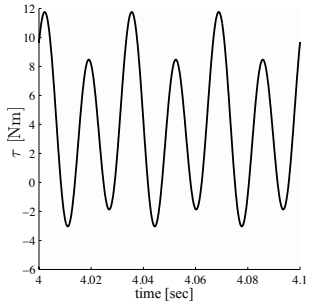

Fig. 9. Torque

## VII. CONCLUSIONS AND FUTURE WORK

We have presented a control systems approach for the analysis and control of a kinematic wobble–yoke Stirling engine mechanism. Due to the mass–spring behavior of the working gas, we have shown that the engine is an unstable linear closed–loop systems where the state feedback is given by the pressure variations in the pistons. By using linear control techniques we designed a pre–compensator that ensure stability of the pistons displacements, and an observer to estimate the piston velocities. Current research is underway to experimentally validate the controllers.

Among the issues that are currently explored are:

- the robustness analysis of the controllers in the presence of parametric uncertainties in the model,
- the energy performance and efficiency of the engine in terms of the mean recoverable mechanical power, and
- the modeling of the regenerator so that pressure drops between the compression and expansion spaces are taken into account.

## REFERENCES


[1] E. García-Canseco, J. M. A. Scherpen, and M. Kuindersma. Modeling for control of a wobble–yoke Stirling engine. In *2009 International Symposium on Nonlinear Theory and its Applications*, pages 544–547, Sapporo, Japan, October 18-21 2009.

[2] G. Smith and S. Barnes. Electrical power generation from heat engines. *Power Electronics for Renewable Energy (Digest No: 1997/170), IEE Colloquium on*, 170:5/1 – 5/6, May 1997.

[3] Smart power foundation. `http://www.smartpowerfoundation.com`.

[4] J. Harrison. Micro combined heat and power (CHP) for housing. In *SET 2004–3rd. Conference on Sustainable Energy Technologies*, Nottingham, UK., Jun 28-30 2004.

[5] Prachi Patel-Predd. Generation cogeneration. *IEEE Spectrum (International Ed.)*, 46(3):56, March 2009.

[6] H. Onovwiona and V. Ugursal. Residential cogeneration systems: review of the current technology. *Renewable and Sustainable Energy Reviews*, 10:389–431, Jan 2006.

[7] W. B. Stine. *Energy Conversion*, chapter Stirling Engines, pages 12.1–12.11. Taylor & Francis Group, LLC, 2007.

[8] T. Finkelstein. *Thermodynamics and Gas Dynamics of the Stirling Cycle Machine by A.J. Organ*, chapter Foreword, pages xvii–xxi. Cambridge University Press, 1992.

[9] R. W. Redlich and D. M. Berchowitz. Linear dynamics of a free–piston Stirling engines. In *Proc. of the Institution of Mechanical Engineers, IMechE*, volume 199, pages 203–213, 1985.

[10] M. D. Kankam and J. S. Rauch. Controllability of free-piston Stirling engine/linear alternator driving a dynamic load. In *28th Intersociety Energy Conversion Engineering Conference*, Atlanta, Georgia, Aug 8-13 1993. ANS, SAE, ACS, IEEE, ASME, AIAA, AIChE.

[11] I. Burrel, S. Leballois, E. Monmasson, and L. Prevond. Energy performance and stability of Stirling micro-cogeneration system. In *Power Electronics and Motion Control Conference 2006, EPE-PEMC*, pages 2057 – 2063, Portoroz, Slovenia, Aug 2006.

[12] G. Benvenuto and F. de Monte. Analysis of free–piston Stirling engine/linear alternator systems: Part 1: Theory. *Journal of Propulsion and Power*, 11(5):1036–1046, October 1995.

[13] G. Benvenuto and F. de Monte. Analysis of free–piston Stirling engine/linear alternator systems: Part 2: Results. *Journal of Propulsion and Power*, 11(5):1047–1055, October 1995.

[14] J. Riofrio, K. Al-Dakkan, M. Hofacker, and E. J. Barth. Control–based design of free–piston Stirling engines. In *American Control Conference 2008*, pages 1533 – 1538, Seattle, Washington, USA, May 2008.

[15] Whispergen heat and power systems. `http://www.whispergen.com`.

[16] D. M. Clucas and J. K. Raine. Development of a hermetically sealed stirling engine battery charger. In *Proc. of the Institution of Mechanical Engineers, IMechC*, volume 208, pages 357–366, Jan 1994.

[17] D. M. Clucas and J. K. Raine. A new wobble drive with particular application in a Stirling engine. In *Proc. of the Institution of Mechanical Engineers, IMechE*, volume 208, pages 337–346, 1994.

[18] E. J. Barth and M. Hofacker. Dynamic modeling of a regenerator for the control–based design of free–piston Stirling engines. In *Proc. of 2009 NSF Engineering Research and Innovation Conference*, Honolulu, Hawai, 2009.

[19] C. H. Chiang. *Kinematics of spherical mechanisms*. Cambridge University Press, (Cambridge [England], New York), 1988.

[20] J. Michael McCarthy. *Geometric Design of Linkages*. Springer, 1 edition, April 2000.

[21] I. Urierli and D. M. Berchowitz. *Stirling Cycle Engine Analysis*. Adam Hilger Ltd, Bristol, 1984.

[22] M. D. Kankam and J. S. Rauch. Comparative survey of dynamic analyses of free–piston Stirling engines. In *26th Intersociety Energy Conversion Engineering Conference*, Boston, Massachussets, August 4-9 1991.

[23] E. D. Rogdakis, N. A. Bormpilas, and I.K. Koniakos. A thermodynamic study for the optimization of stable operation of free–piston Stirling engines. *Energy Conversion & Management*, 45:575–593, 2004.

[24] Gene F. Franklin, J. David Powell, and Abbas Emami-Naeini. *Feedback control of dynamic systems*. Person–Prentice Hall, 4th edition, 2002.


## APPENDIX
## PARAMETERS OF THE MODEL

$$\beta_1 = \frac{1}{T_k}\left(V_{dc} + \frac{V_{swc}}{2}\right) + \frac{1}{T_h}\left(V_{de} + \frac{V_{swe}}{2}\right) + \frac{V_k}{T_k} + \frac{V_r}{T_r} + \frac{V_h}{T_h}. \tag{A.1}$$

$$\beta_2 = \frac{8p_m T_h^2 \beta_1 (A_p - A_r)}{T_k (A_p h_s - 4T_h\beta_1)^2}, \quad \beta_3 = -\frac{8p_m T_h A_p \beta_1}{(A_p h_s - 4T_h\beta_1)^2}, \tag{A.2}$$

$$\beta_4 = \frac{8p_m T_k^2 A_p \beta_1}{(4T_k\beta_1 + (A_p - A_r)h_s)^2 T_h}, \tag{A.3}$$

$$\beta_5 = \frac{8p_m T_k \beta_1 (A_p - A_r)}{(4T_k\beta_1 + (A_p - A_r)h_s)^2}, \tag{A.4}$$

$$\beta_6 = -\frac{8p_m T_h^2 \beta_1 (A_p - A_r)}{(A_p h_s + 4T_h\beta_1)^2 T_k}, \quad \beta_7 = \frac{8p_m T_h A_p \beta_1}{(A_p h_s + 4T_h\beta_1)^2}, \tag{A.5}$$

$$\beta_8 = -\frac{8p_m T_k^2 A_p \beta_1}{(-4T_k\beta_1 + (A_p - A_r)h_s)^2 T_h}, \tag{A.6}$$

$$\beta_9 = -\frac{8p_m T_k \beta_1 (A_p - A_r)}{(-4T_k\beta_1 + (A_p - A_r)h_s)^2} \tag{A.7}$$